Lipids (2019)
DOI 10.1002/lipd.12197

ORIGINAL ARTICLE

Acute Hypercapnia/Ischemia Alters the Esterification of Arachidonic Acid and Docosahexaenoic Acid Epoxide Metabolites in Rat Brain Neutral Lipids

Yurika Otoki[1,2] · Adam H. Metherel[3] · Theresa Pedersen[1] · Jun Yang[4,5] · Bruce D. Hammock[4,5,6] · Richard P. Bazinet[3] · John W. Newman[6,7,8] · Ameer Y. Taha[1,6]

Received: 26 March 2019 / Revised: 27 August 2019 / Accepted: 28 August 2019

Abstract In the brain, approximately 90% of oxylipins are esterified to lipids. However, the significance of this esterification process is not known. In the present study, we (1) validated an aminopropyl solid phase extraction (SPE) method for separating esterified lipids using 100 and 500 mg columns and (2) applied the method to quantify the distribution of esterified oxylipins within phospholipids (PL) and neutral lipids (NL) (i.e. triacylglycerol and cholesteryl ester) in rats subjected to head-focused microwave fixation (controls) or CO_2-induced hypercapnia/ischemia. We hypothesized that oxylipin esterification into these lipid pools will be altered following CO_2-induced hypercapnia/ischemia. Lipids were extracted from control ($n = 8$) and CO_2-asphyxiated ($n = 8$) rat brains and separated on aminopropyl cartridges to yield PL and NL. The separated lipid fractions were hydrolyzed, purified with hydrophobic–lipophilic–balanced SPE columns, and analyzed with ultra-high-pressure liquid chromatography coupled to tandem mass spectrometry. Method validation showed that the 500 mg (vs 100 mg) aminopropyl columns yielded acceptable separation and recovery of esterified fatty acid epoxides but not other oxylipins. Two epoxides of arachidonic acid (ARA) were significantly increased, and three epoxides of docosahexaenoic acid (DHA) were significantly decreased in brain NL of CO_2-asphyxiated rats compared to controls subjected to head-focused microwave fixation. PL-bound fatty acid epoxides were highly variable and did not differ significantly between the groups. This study demonstrates that hypercapnia/ischemia alters the concentration of ARA and DHA epoxides within NL, reflecting an active turnover process regulating brain fatty acid epoxide concentrations.

Keywords Arachidonic acid and docosahexaenoic acid epoxides · Eicosanoids · Esterified oxylipins · Hypercapnia/ischemia · Rat brain · Turnover

Lipids (2019).

Supporting information Additional supporting information may be found online in the Supporting Information section at the end of the article.

✉ Ameer Y. Taha
ataha@ucdavis.edu

1 Department of Food Science and Technology, College of Agriculture and Environmental Sciences, University of California, One Shields Avenue, Davis, CA 95616, USA

2 Food and Biodynamic Laboratory, Graduate School of Agricultural Science, Tohoku University, Sendai, Miyagi, Japan

3 Department of Nutritional Sciences, Faculty of Medicine, University of Toronto, ON, M5S 1A8, Canada

4 Department of Entomology and Nematology, College of Agriculture and Environmental Sciences, University of California, Davis, CA 95616, USA

5 Comprehensive Cancer Center, Medical Center, University of California, Davis, CA 95616, USA

6 West Coast Metabolomics Center, Genome Center, University of California–Davis, Davis, CA 95616, USA

7 Department of Nutrition, University of California–Davis, Davis, CA 95616, USA

8 United States Department of Agriculture, Agricultural Research Service, Western Human Nutrition Research Center, Davis, CA 95616, USA

Abbreviations

ALA	α-linolenic acid
ARA	arachidonic acid
BHT	butylated hydroxytoluene

CE	cholesteryl ester
COX	cyclooxygenase
CYP	cytochrome p450
DAG	diacylglycerols
DHA	docosahexaenoic acid
DiHETE	dihydroxyeicosatetraenoic acid
DiHETrE	dihydroxyeicosatrienoic acid
DiHOME	dihydroxyoctadecenoic acid
DPPC	1,2-dipalmitoyl-sn-glycero-3-phosphocholine
EDTA	Ethylenediaminetetraacetic acid
EPA	eicosapentaenoic acid
EpDPE	epoxydocosapentaenoic acid
EpETE	epoxyeicosatetraenoic acid
EpETrE	epoxyeicosatrienoic acid
EpOME	epoxyoctadeenoic acid
FFA	unesterified fatty acids
GC	gas chromatography
HDoHE	hydroxydocosahexaenoic acid
HEPE	hydroxyeicosapentaenoic acid
HETE	hydroxyeicosatetraenoic acid
HETrE	hydroxyeicosatrienoic acid
HODE	hydroxyoctadecadienoic acid
HOTrE	hydroxyoctadecatrienoic acid
LNA	linoleic acid
LOQ	limits of quantitation
LOX	lipoxygenase
LT	leukotriene
LysoPL	lysophospholipids
NL	neutral lipids
oxo-ETE	oxo-eicosatetraenoic acid
oxo-ODE	oxo-octadecadienoic acid
PG	prostaglandin
15-PGDH	15-hydroxyprostaglandin dehydrogenase
PL	phospholipids
PUFA	polyunsaturated fatty acids
sEH	soluble epoxide hydrolase
SPE	solid phase extraction
TAG	triacylglycerols
TPP	triphenylphosphine
TXB2	tromboxane B2
UPLC–MS/MS	ultra-high-pressure liquid chromatography tandem mass spectrometry
TriHOME	trihydroxyoctadecenoic acid.

Introduction

Polyunsaturated fatty acids (PUFA) are precursors to hundreds of bioactive lipid mediators known as oxylipins. PUFA can be converted into oxylipins *via* auto-oxidation or a host of enzymes, including cyclooxygenase (COX) (Funk, 2001; Laneuville et al., 1995), lipoxygenase (LOX) (Chang et al., 2015; Murphy et al., 1995), cytochrome p450 (CYP) (Arnold et al., 2010; Fer et al., 2008a, b), 15-hydroxyprostaglandin dehydrogenase (15-PGDH) (Snyder et al., 2015; Wendell et al., 2015), and soluble epoxide hydrolase (sEH) enzymes (Greene et al., 2000; Inceoglu et al., 2007).

In peripheral tissue and brain, oxylipins regulate multiple biological processes, including angiogenesis (Rand et al., 2017), vasodilation (Inceoglu et al., 2012; Liu et al., 2011), vasoconstriction (Dabertrand et al., 2013), signaling (Hennebelle et al., 2017), inflammation (Rey et al., 2016), and the resolution of inflammation (Levy et al., 2001; Orr et al., 2013; Serhan et al., 2002). In particular, CYP-derived epoxides of n-6 arachidonic acid (ARA, 20:4n-6) and n-3 eicosapentaenoic acid (EPA, 20:5n-3) and docosahexaenoic acid (DHA, 22:6n-3) have been reported to suppress brain inflammation, promote resolution, and increase axonal outgrowth (Abdu et al., 2011; Vito et al., 2014).

In the brain (and other tissues), the majority of PUFA, such as ARA and DHA, are esterified to membrane phospholipids (PL), where they undergo rapid turnover (acylation/deacylation) (Rapoport, 1996; Robinson and Rapoport, 1989) *via* the "Lands Pathway" (Lands and Merkl, 1963). Neuroreceptor-coupled phospholipase A_2 activation or brain injury (e.g. ischemia) induces the release of bound PUFA (Bazan Jr., 1970; Ramadan et al., 2011; Taha et al., 2014), resulting in an increase in unesterified fatty acids (FFA) (Bazan Jr., 1970) and their COX-, LOX-, 15-PGDH-, CYP-, or sEH-derived metabolites (Hennebelle et al., 2017, 2019). PUFA-derived oxylipins exert their biological effects when present in the unesterified (i.e. free) form (Lahvic et al., 2018; Obinata et al., 2005). In the brain, however, the majority of oxylipins (up to approximately 90%) are esterified, presumably to lipids (Taha et al., 2018). The type of lipids they are esterified to and how this process is regulated in the brain are not known.

Previous studies have shown that oxylipins esterified to PL or neutral lipids (NL) composed mainly of triacylgycerols (TAG) and cholesteryl esters (CE), can be liberated *via* lipase enzymes (Chaitidis et al., 1998; Morrow et al., 1992; Wang et al., 2009) following the induction of inflammatory pathways by FFA addition to cell culture or carbon tetrachloride injection to rats (Morrow et al., 1992; Wang et al., 2009). The formation of esterified oxylipins was reported to occur *via* direct auto- or LOX-mediated oxidation of PUFA esterified to PL (Chaitidis et al., 1998; Morrow et al., 1992). Recently, however, Klett et al. reported that, *in vitro*, unesterified ARA-derived hydroxyeicosatetraenoic acids (HETE) and epoxyeicosatrienoic acids (EpETrE) can be esterified to lysophospholipids following their acylation by acyl-CoA synthetase (Klett et al., 2017). This is consistent with studies showing that labeled HETE incorporate into NL or PL of human polymorphonuclear leukocytes and isolated neutrophils and platelets (Brezinski

and Serhan, 1990; Joulain et al., 1995; Stenson and Parker, 1979a), and EpETrE incorporate into the PL of mastocytoma cells (Bernstrom et al., 1992) and isolated porcine coronary artery and endothelial cells (Fang et al., 2003).

A recent study by Liu et al. showed an alternative pathway for oxidized PL formation, where LOX oxidizes lysophospholipids containing ARA at the sn-2 position to form 15-HETE lysophospholipid, which is then esterified to a saturated fatty acid *via* an sn-1 acyltransferase (Liu et al., 2019). The formation of oxidized PL *via* this pathway was upregulated following thrombin treatment of platelets (Liu et al., 2019).

Others reported direct and increased esterification of HETE and EpETrE into PL or NL following pharmacological stimulation of polymorphonuclear leukocytes or isolated neutrophils and platelets (Brezinski and Serhan, 1990; Stenson and Parker, 1979b). Collectively, these studies suggest that, *in vivo*, oxylipins may incorporate into PL and NL pools via multiple regulated pathways, consistent with evidence showing that the majority of oxylipins in rat brain are esterified (Taha et al., 2018).

In the present study, we first confirmed the validity of an established aminopropyl column method used to isolate oxylipins esterified to PL and NL (Grapov, 2012; Wang et al., 2009), and then applied the method to test whether esterified oxylipin pools are altered in rat brain following CO_2-induced hypercapnia/ischemia. We hypothesized that, similar to well-established processes governing the lipase-mediated release of esterified oxylipins during inflammation (Morrow et al., 1992; Wang et al., 2009), ischemia-induced brain injury would increase the esterification of free oxylipins into various lipid pools. This article provides evidence in support of the hypothesis, suggesting the existence of a turnover pathway guiding the release and esterification of unesterified oxylipins *in vivo*.

Materials and Methods

Materials

Fatty acid standards were purchased from Nu-chek Prep Inc. (Elysian, MN, USA). PL standards were purchased from Avanti Polar Lipids (Alabaster, AL, USA). Seventy-two oxylipin standards, listed in Supplementary Table 1, and their deuterated surrogate standards (nine in total) were purchased from Cayman Chemical (Ann Arbor, MI, USA) or Larodan (Monroe, MI, USA). All solvents were LC–MS grade and were purchased from Fisher Scientific (Santa Clara, CA, USA). Concentrated HCl (ACS reagent, 37%) for fatty acid transesterification reactions was purchased from Sigma Aldrich (St. Louis, MO, USA)

Ischemia Study

Animals

All procedures were performed in accordance with the policies of the Canadian Council on Animal Care and were approved by the Animal Ethics Committee of the University of Toronto.

In the present study, we used the entire left hemisphere (containing cerebrum, cerebellum, and brainstem) of rats from a recently published study that compared the effects of CO_2-induced hypercapnia/ischemia and high-energy microwave fixation on free oxylipin concentrations (Hennebelle et al., 2019). In brief, 1-month-old Long Evans male rats were purchased from Charles River (Saint-Constant, QC, Canada) and housed in pairs. The rats were fed *ad libitum* for 30 days with a rat chow diet containing 6.2% fat by weight (2018 Teklad Global, 18% protein rodent diet; Envigo, Madison, WI, USA). The fatty acid composition of the diet (% of total fatty acids) was 18.5% palmitic acid (16:0), 2.8% stearic acid (18:0), 18.5% oleic acid (18:1 n-9), 54.8% linoleic acid (LNA; 18:2 n-6), and 5.6% α-linolenic acid (ALA; 18:3 n-3) (Trepanier et al., 2012).

Experiments were performed after the animals were housed at our facility for approximately one month (i.e. day 60 onward) to (1) minimize the potential effects of hormonal changes associated with puberty occurring at ~42 days of age in this strain of rats (Ge et al., 2007) and (2) to acclimatize the animals to the Teklad Global diet provided in the facility, which differs in fatty acid composition from the diet at Charles River. The Charles River diet contains fish meal, whereas the Teklad Global diet is based on plant oils.

Rats ($n = 8$) were subjected to head-focused microwave fixation (13.5 kW for 1.6 s, Cober Electronics Inc., Norwalk, CT, USA) to halt brain lipid metabolism or CO_2 asphyxiation for 2 min ($n = 8$) to induce global brain hypercapnia/ischemia. The heads were decapitated, and the brains were excised within 6.5 min, flash frozen in liquid nitrogen, and stored in a −80°C freezer. Samples were shipped on dry ice from Toronto, ON, Canada to Davis, CA, USA, where they were maintained in a −80 °C freezer until they were analyzed.

Validation of the NL and PL Separation Method

The PL and NL separation method was validated using an aminopropyl column (particle size 40 μm; Agilent Bond Elut NH_2, Agilent Corporation, Palo Alto, CA, USA) as previously described (Grapov, 2012; Wang et al., 2009). The separation of PL, CE, TAG, and FFA lipid standards and free oxylipin standards was tested using two sizes of aminopropyl columns—100 and 500 mg. The accuracy of

Table 1 Solid phase extraction (SPE) protocol used to separate NL, FFA, and PL on 100 and 500 mg aminopropyl columns

Extraction steps	Solvents/Samples	Volume of solvents	
		100 mg columns	500 mg columns
Conditioning	Methanol	2 mL	6 mL
	Water	2 mL	6 mL
	0.1 M aq. HCl	2 mL	6 mL
	Water	4 mL	12 mL
	Methanol	2 mL	6 mL
	Hexane	6 mL	18 mL
Loading samples	Lipids	0.2 mg	1 mg
NL elution	Hexane	2.5 mL	7.5 mL
	Hexane:chloroform:ethylacetate (100:5:5, v:v:)	2 mL	6 mL
FFA elution	Chloroform:Isopropanol (2:1, v:v)	2 mL	6 mL
Wash	Acetic acid:diethyl ether (2:98, v:v)	2 mL	6 mL
PL elution	Acetic acid:methanol (10:90, v:v)	5 mL	15 mL

FFA, unesterified fatty acids; NL, neutral lipids; PL, phospholipids.

the method was also assessed on one rat brain hemisphere using both columns.

Separation of PL, CE, TAG, and FFA Standards with Aminopropyl Columns

The elution of free and esterified lipid standards was tested using the 100 and 500 mg solid phase extraction (SPE) columns. Our goal was to determine the optimal column filter material and solvent volumes that would separate the lipid fractions (smaller columns require less solvent). The solvent elution sequence and volumes used for each column size are presented in Table 1. As shown, the columns were first preconditioned by gravity elution with methanol, water, 0.1 M HCl, and hexane. The 100 and 500 mg aminopropyl columns were then loaded with 0.2 and 1 mg, respectively, of each of the following lipid standards dissolved in 100 µL chloroform: unesterified palmitic acid, cholesteryl palmitate, tripalmitin, or 1,2-dipalmitoyl-sn-glycero-3-phosphocholine (DPPC). Hence, each standard was applied separately to each of the 100 and 500 mg columns (i.e. four standards at 0.2 mg each, applied separately to the 100 mgs column and four standards at 1 mg each, applied separately to the 500 mgs column—total of eight columns). Standard purity was confirmed by gas chromatography (GC) coupled to flame-ionization detection prior to loading them on the columns. NL containing tripalmitin and cholesteryl palmitate were eluted with hexane and hexane:chloroform:isopropanol (100:5:5). FFA were eluted with chloroform:isopropanol (2:1, v/v). PL were eluted with 10% acetic acid in methanol (v/v) after washing the columns with diethyl ether containing 2% acetic acid.

The lipid fractions (PL, NL, and FFA) were collected from each column, dried under nitrogen, and reconstituted in 400 µL toluene. Unesterified heptadecanoic acid was added to the collected unesterified fraction; triheptadecanoin was added to the collected cholesteryl palmitate and tripalmitin fractions (which elute in the NL fraction); and diheptanoyl phosphatidylcholine was added to the collected DPPC fraction. The amount of heptadecanoic acid standard added to each of the free palmitate-, tripalmitin-, and DPPC fractions eluted by the 100 and 500 mg aminopropyl columns was 0.04 and 0.2 mg, respectively. The amount of triheptadecanoin added to cholesteryl palmitate fractions was 0.02 and 0.1 mg for the 100 and 500 mg columns, respectively.

The eluted lipids in each fraction were transesterified by adding 3 mL methanol and 600 µL of 8% concentrated HCl in methanol and heating them at 90 °C for 1 h. After cooling, 1 mL of hexane and 1 mL of water were added. The samples were vortexed and allowed to sit undisturbed for 10 min to enable separation of the hexane and aqueous phases. A total of 900 µL of the upper hexane layer containing the fatty acid methyl esters were transferred to a new tube containing 450 µL water. Samples were vortexed and centrifuged for 2 min at 15,871 ×*g*. The upper hexane layer was dried under nitrogen, reconstituted in 100 µL hexane, and transferred to amber GC vials containing inserts.

Fatty acids methyl esters were analyzed on a Perkin Elmer Clarus 500 GC system (Perkin Elmer, Richmond, CA, USA) equipped with a FFAP-fused silica capillary column (Length: 30 m, Inner Diameter: 0.25 mm, Film thickness: 0.25 µm; Agilent Technologies, Santa Clara, CA, USA). The injector temperature was set at 240 °C and the detector at 300 °C. Helium was used as a carrier gas at a constant flow rate of 1.3 mL/min. The oven temperature was set at 80 °C for 2 min, increased to 185 °C by 10 °C/

min and to 240 °C by 5 °C/min, and maintained at 240 °C for 13 min. Fatty acids were identified based on the retention times of a custom mix of 29 fatty acid methyl ester standards.

Fatty acid and internal standard (heptadecanoic acid) peak areas were used to determine the amount (nmol) of free or esterified palmitic acid standard collected in each lipid pool (FFA, PL, and NL). They were added to determine the total amount of fatty acids per fraction and the sum was divided by the actual amount we added to the column to determine percent recovery, as follows:

$$\text{Percent recovery}\,(\%) = \frac{\sum \text{Amount}\,(\text{nmol})\ \text{in each eluted fraction}}{\text{Amount}\,(\text{nmol})\text{added to the column}} \times 100$$

Determination of Free Oxylipin Elution Profile on the Aminopropyl Columns

A mixture of 72 free oxylipin standards (listed in Supplementary Table 1), ranging in amount between 2.5 and 62.5 pmol, was loaded onto both aminopropyl columns ($n = 1$ per column) to confirm that free oxylipins eluted with the FFA fraction. The elution sequence described in Table 1 was applied, and NL, FFA, and PL fractions were collected. Each fraction was dried under nitrogen and reconstituted in 200 μL methanol containing 0.1% acetic acid and 0.1% butylated hydroxytoluene (BHT), 10 μL of antioxidant mix (0.2 mg/mL BHT, ethylenediaminetetraacetic acid [EDTA] and triphenylphosphine [TPP] in methanol: water, 1:1, v:v) after being spiked with 10 μL surrogate standard solution containing 2 μM of d11-11(12)-EpETrE, d11-14,15-DiHETrE, d4-6-keto-PGF1α, d4-9-HODE, d4-LTB4, d4-PGE2, d4-TXB2, d6-20-HETE, and d8-5-HETE in methanol. d4-PGE2 was only used for quantifying free oxylipins with similar retention times on the LC column, specifically LNA-derived trihydroxylated metabolites (9,10,13-TriHOME and 9,12,13-TriHOME), prostanoids (15-deoxy-PGJ2, PGF2-alpha, PGB2, PGD2, PGD3, PGE1, PGE2, PGE3 and PGJ2), and the hydroxylated EPA metabolite Resolvin E1. Retention times for each compound are provided in Supplementary Table 1. d4-PGE2 was not used to quantify esterified concentrations of these metabolites because it degrades during the hydrolysis process.

Ultrapure water (1.8 mL) was added to the samples, which were then loaded onto the 60 mg Oasis HLB columns. All columns prerinsed with one volume of ethyl acetate and two volumes of methanol and preconditioned with two volumes of SPE buffer containing 5% methanol and 0.1% acetic acid in ultrapure Millipore water (Hennebelle et al., 2017). The columns were rinsed twice with SPE buffer before being subjected to 20 min of vacuum (≈20 psi). Oxylipins were eluted with 0.5 mL methanol and 1.5 mL ethyl acetate in 2 mL centrifuge tubes. Samples were dried under nitrogen, reconstituted in 100 μL methanol, and subjected to mass spectrometry analysis (ultra-high-pressure liquid chromatography tandem mass spectrometry [UPLC–MS/MS]) as described below. Quantitation was achieved using the surrogate standard after correcting for the response factor using a calibration curve for each oxylipin.

The percent recovery of each oxylipin within PL, NL, or FFA separated by the aminopropyl columns was calculated as follows:

$$\text{Percent recovery}\,(\%) = \frac{\sum \text{Amount}\,(\text{nmol})\text{detected in each eluted fraction}}{\text{Amount}\,(\text{nmol})\ \text{added to the column}} \times 100$$

Brain Extract Fractionation

The separation efficiency of esterified oxylipins with both columns (100 and 500 mg) was tested on one rat brain hemisphere and compared. Total lipids were extracted using a modified Folch procedure (Trepanier et al., 2012). Approximately 800 mg of a rat brain sample were homogenized in 5 mL methanol containing 0.01% BHT. Five mL of methanol and 20 mL of chloroform were then added to reach a final chloroform:methanol ratio of 2:1. The samples were vortexed, and 7.5 mL of 0.1 M NaCl were added. The samples were vortexed again and centrifuged at 730 ×*g* for 5 min. The bottom chloroform layer containing total lipids was transferred to a new tube. The lipid extraction process was repeated by adding 15 mL of chloroform, centrifuging, and pooling the bottom chloroform layer with the first one. The chloroform extract was dried under nitrogen and reconstituted in 8 mL chloroform (or approximately 10 mg of fat/mL chloroform on the basis that the brain contains ~10% fat).

A total of 20 μL of total lipid extract containing ~0.2 mg lipid was loaded onto the 100 mg column; 100 μL of total lipid extract containing ~1 mg lipid was loaded onto the 500 mg column. NL, PL, and FFA were separated using the solvent elution sequence and volumes detailed in Table 1. All collected fractions were dried under nitrogen and reconstituted in 200 μL methanol containing 0.1% acetic acid and 0.1% BHT, 10 μL of antioxidant mix, and 10 μL surrogate standard solution. Esterified oxylipins from PL and NL fractions were hydrolyzed in 200 μL of 0.25 M sodium carbonate in methanol/water (1:1) at 60 °C for 30 min. The samples were cooled at room temperature, and 25 μL of acetic acid and 1575 μL of Millipore water were added prior to SPE (60 mg Oasis HLB columns). Free

oxylipins collected in the FFA fraction were diluted with 1.8 mL ultrapure water and directly purified with 60 mg Oasis HLB 3cc columns (Waters, Milford, MA, USA). SPE columns were prerinsed with one volume of ethyl acetate and two volumes of methanol and preconditioned with two volumes of SPE buffer containing 5% methanol and 0.1% acetic acid in ultrapure Millipore water, as described above. The columns were rinsed twice with SPE buffer and subjected to 20 min of vacuum to dry (≈20 psi). Oxylipins were eluted with 0.5 mL methanol and 1.5 mL ethyl acetate, reconstituted in 100 µL methanol, filtered by centrifugation using Ultrafree-MC centrifugal filters (0.1 µm; Millipore, Bedford, MA, USA), and subjected to UPLC–MS/MS analysis (see below). Oxylipins were quantitated using the surrogate standard (to correct for losses during the extraction), after adjusting for the response factor of each oxylipin using a calibration curve.

Esterified Oxylipin Analysis of Rat Brain Subjected to Microwave Fixation or CO_2-Induced Hypercapnia/ Ischemia

Because the 500 mg aminopropyl columns yielded better results than the 100 mg columns (see Results), they were used to separate total lipid extracts from the rat brain samples subjected to high-energy microwave fixation or CO_2-induced hypercapnia/ischemia ($n = 8$ per group). Total lipids were first extracted with chloroform/methanol (2:1 v/v) using a modified Folch procedure utilizing lower solvent volumes (Folch et al., 1957). Approximately 680–1028 µL of precooled 0.9% KCl (w/v) solution containing 1 mM of EDTA was added to an equal mass (680–1028 mg) of frozen brain tissue (one hemisphere), yielding a 50% mixture (w/v). The samples were homogenized with zirconia beads in a Bullet Blender (Next Advance, Troy, NY, USA). A total of 600 µL of the 50% homogenate mixture was mixed with 600 µL of 0.9% KCl (w/v) aqueous solution containing 1 mM of EDTA, and 4.8 mL of chloroform: methanol (2:1, v/v) containing 0.002% BHT. The extract was centrifuged at 1000 ×*g* for 10 min at 4 °C. The lower chloroform layer containing total lipids was collected. The remaining aqueous layer containing a semisolid interface was re-extracted with chloroform:methanol (10:1, v/v). The mixture was vortexed and centrifuged at 1000 ×*g* for 10 min at 4 °C. The lower chloroform layer was combined with the first chloroform extract and dried under nitrogen gas. The dried extract was redissolved in 3 mL of chloroform.

PL and NL in 100 µL chloroform were separated using the 500 mg aminopropyl SPE column and were hydrolyzed and purified with the 60 mg Oasis HLB column as described above (for the brain test sample).

UPLC–MS/MS Analysis

Oxylipins were analyzed within a week following extraction to minimize the potential impact of prolonged storage on lipid oxidation. The samples were stored in a −80 °C freezer during this period. Seventy-two oxylipins were analyzed on an Agilent 1290 LC (Agilent Corporation) coupled to an Agilent 6460 Triple Quadrupole MS (Agilent Corporation). Oxylipin species were separated on an Agilent Eclipse Plus C18 column (2.1 × 150 mm, 1.8 µm, Agilent Corporation) with a binary gradient consisting of solvent A (water containing 0.1% acetic acid) and solvent B (Acetonitrile: methanol 80:15 containing 0.1% acetic acid). The autosampler temperate was 4 °C and the column temperature was maintained at 45 °C. The gradient profile is shown in Supplementary Table 2. Oxylipins were ionized with negative-mode electrospray ionization. The ion source gas temperature was 250 °C, gas flow was 10 L/min, sheath gas temperature was 300 °C, sheath gas flow was 11 mL/min, nebulizers were at 35 psi, and the capillary gas was at 3500 V/-3500 V. Optimization parameters and ion pairs for each oxylipin are described in Supplementary Table 1. Oxylipins were detected using dynamic multiple reaction monitoring mode.

Statistical Analysis

All data are expressed as mean ± SD. Differences between the 100 and 500 mg columns were assessed using an unpaired *t*-test (GraphPad Prism 7.04, La Jolla, CA, USA). Differences between the head-focused microwave fixation and CO_2 hypercapnia/ischemia groups were assessed on GraphPad Prism with an unpaired *t*-test or Mann–Whitney U test depending on whether the data were normally distributed or not based on Shapiro–Wilk's test. Oxylipins with more than 70% values above the limits of quantitation (LOQ) ina given group were analyzed. For these oxylipins, missing values were imputed by dividing the LOD by the square root of 2. Statistical significance was set at $p < 0.05$.

Results

Lipid Class Separation

The purity of the unesterified palmitic acid, cholesteryl palmitate, tripalmitin, and DPPC were verified by GC. All standards were over 98% pure (Supplementary Table 3).

Table 2 Percent recovery of unesterified and esterified palmitate within FFA, NL, and PL separated with 100 or 500 mg aminopropyl columns ($n = 1$ per standard per column)

	100 mg column			500 mg column		
	NL (%)	FFA (%)	PL (%)	NL (%)	FFA (%)	PL (%)
Palmitic acid (FFA)	3	93	3	8	92	1
Cholesteryl-palmitate (CE)	82	5	6	105	3	3
Tripalmitin (TAG)	109	2	2	101	1	1
DPPC (PL)	22	3	102	4	1	92

Abbreviations: CE, cholesteryl esters; DPPC, 1,2-dipalmitoyl-sn-glycero-3-phosphocholine; FFA, unesterified fatty acids; TAG, triacylglycerols; NL, neutral lipids; PL, phospholipids. $n = 1$ for CE, DPPC, FFA, and TAG standards applied to each of the two columns.

The remaining <2% impurities consisted of palmitoleic acid and an unknown peak at 10.5 min in all fractions.

Table 2 shows the percent recovery of unesterified and esterified palmitate following separation with the 100 and 500 mg aminopropyl columns. As shown, 93% and 92% of unesterified palmitate were retained in the FFA fraction collected from the 100 and 500 mg columns, respectively. The NL fraction collected from the 100 and 500 mg columns contained 82% and 105% of the added cholesteryl palmitate, respectively. It also contained 109% (100 mg column) and 101% (500 mg column) of the added tripalmitin (i.e. TAG). The PL fraction retained 102% of the added DPPC on the 100 mg column and 92% on the 500 mg column. Thus, both columns separated free and esterified fatty acid standards, but the 500 mg column yielded greater recovery of esterified lipids (92–105%) compared to the 100 mg column (82–109%).

GC analysis also showed the presence of other fatty acids in the separated FFA, NL, and PL, which appear to have originated from the columns (Supplementary Table 4). However, none of the detected fatty acids (stearic (18:0), oleic (18:1 n-9), linoleic (18:2 n-6), and α-linolenic (18:3 n-3) acid) served as precursors to long-chain PUFA oxylipins of interest or those that were well separated by the columns (see next section).

Partition of Free Oxylipin Standards

Table 3 shows the percent recovery of 72 unesterified oxylipin standards, applied directly to each of the 100 and 500 mg aminopropyl columns, within FFA, NL, and PL. Our goal here was to ensure that free oxylipins eluted in the FFA fraction.

Total % recovery of free epoxy, hydroxy, and ketone PUFA metabolites, reflecting the total amount obtained in each fraction relative to the amount applied to the column, ranged from 5% to 90%. The majority of what was recovered from the columns (>90%) was found in the FFA fraction, suggesting similar polarity of epoxy, hydroxy, and ketone oxylipins to FFA. However, there were a few exceptions. These were LNA-derived 9(10)-EpOME and AA-derived 15-oxo-eicosatetraenoic acid (oxo-ETE) separated with the 100 mg column, and LNA-derived 12(13)-EpOME separated with both columns. 9(10)-EpOME and 12(13)-EpOME showed some recovery in NL (16–24%). More 15-oxo-ETE was retained in NL (7%) than in FFA (5%).

Total recovery of prostaglandins, leukotrienes (LT), thromboxanes, dihydroxy, and trihydroxy metabolites was low, and the separation was inefficient, meaning that many did not end up in the FFA fraction. Their recovery ranged between 24% and 76% on the 100 mg column and between 20% and 84% on the 500 mg column. Dihydroxy metabolites eluted in FFA and PL, whereas prostaglandins, LT, thromboxanes, and trihydroxy metabolites eluted almost exclusively with PL.

Analysis of Brain Samples with the 100 and 500 mg Aminopropyl Columns

Total lipids extracted from one brain hemisphere of a CO_2-asphyxiated rat were separated with each of the 100 and 500 mg aminopropyl columns in order to explore the variance associated with separating oxylipins esterified to NL and PL with each column ($n = 3$/column). NL and PL were collected, hydrolyzed after adding deuterated surrogate standards, and quantified by UPLC–MS/MS. The means, SD, and coefficients of variation for each column are presented in Table 4. As shown, the coefficients of variation for oxylipins bound to NL and PL were much lower with the 500 mg aminopropyl columns compared to the 100 mg columns. More oxylipins were detected in NL when using the 500 mg column compared to the 100 mg column, likely because more total lipids were loaded onto the 500 mg column (~1 mg) than the 100 mg column (~0.2 mg), resulting in an enhanced signal on the UPLC–MS/MS.

For detected compounds, concentrations of esterified ARA- and DHA-derived epoxides within NL and PL did

Table 3 Percent recovery of unesterified oxylipins within the different lipid fractions following separation with the 100 and 500 mg aminopropyl columns ($n = 1$ per column)

		100 mg column				500 mg column			
		Total recovery (%)	Recovery per fraction (%)[a]			Total recovery (%)	Recovery per fraction (%)[a]		
			In FFA (%)	In NL (%)	In PL (%)		In FFA (%)	In NL (%)	In PL (%)
Epoxy-	9(10)-EpOME	96	80	16	0	118	109	9	0
	12(13)-EpOME	120	96	24	0	164	143	20	0
	5(6)-EpETrE	27	25	2	0	31	31	0	0
	8(9)-EpETrE	76	68	8	0	72	64	8	0
	11(12)-EpETrE	74	66	8	0	77	77	0	0
	14(15)-EpETrE	68	60	9	0	78	71	7	0
	8(9)-EpETE	79	73	6	0	90	90	0	0
	11(12)-EpETE	76	76	0	0	85	85	0	0
	14(15)-EpETE	84	75	9	0	83	83	0	0
	17(18)-EpETE	62	62	0	0	78	78	0	0
	7(8)-EpDPE	81	81	0	0	53	53	0	0
	10(11)-EpDPE	73	68	5	0	71	70	1	0
	13(14)-EpDPE	70	65	5	0	74	74	0	0
	16(17)-EpDPE	70	70	0	0	66	66	0	0
	19(20)-EpDPE	60	60	0	0	59	59	0	0
Dihydroxy-	9,10-DiHOME	44	31	0	14	52	26	0	27
	12,13-DiHOME	54	48	0	7	63	40	0	23
	5,6-DiHETrE	54	0	0	54	46	0	0	46
	8,9-DiHETrE	38	3	0	35	50	0	0	50
	11,12-DiHETrE	37	25	0	13	41	13	0	28
	14,15-DiHETrE	46	39	0	7	52	30	0	22
	5,15-DiHETE	32	0	0	32	24	0	0	24
	8,15-DiHETE	24	24	0	0	23	23	0	0
	5,6-DiHETE	42	0	0	42	20	0	0	20
	14,15-DiHETE	37	37	0	0	46	20	0	26
	17,18-DiHETE	50	29	0	20	72	26	0	46
Hydroxy-	9-HODE	70	66	1	2	63	59	1	2
	13-HODE	63	60	1	2	59	57	0	2
	15(S)-HETrE	72	70	2	0	84	84	0	0
	5-HETE	10	10	0	0	6	6	0	0
	8-HETE	58	58	0	0	50	50	0	0
	9-HETE	60	60	0	0	59	59	0	0
	11-HETE	73	73	0	0	69	68	0	1

(Continues)

Table 3 Continued

		100 mg column				500 mg column			
		Total recovery (%)	Recovery per fraction (%)[a]			Total recovery (%)	Recovery per fraction (%)[a]		
			In FFA (%)	In NL (%)	In PL (%)		In FFA (%)	In NL (%)	In PL (%)
	12-HETE	65	64	1	0	65	65	0	0
	15-HETE	72	70	1	0	64	64	0	0
	20-HETE	66	66	0	0	55	55	0	0
	9-HOTrE	49	49	0	0	47	47	0	0
	13-HOTrE	65	65	0	0	62	62	0	0
	5-HEPE	10	10	0	0	5	5	0	0
	8-HEPE	51	51	0	0	43	43	0	0
	12-HEPE	65	65	0	0	63	63	0	0
	15-HEPE	66	66	0	0	63	63	0	0
	17-HDoHE	60	60	0	0	40	40	0	0
Ketone	9-oxo-ODE	26	26	0	0	43	43	0	0
	13-oxo-ODE	0	0	0	0	41	41	0	0
	5-oxo-ETE	21	21	0	0	27	27	0	0
	12-oxo-ETE	0	0	0	0	0	0	0	0
	15-oxo-ETE	12	5	7	0	13	13	0	0
Prostaglandins, leukotrienes, thromboxanes, and other metabolites	20-COOH-LTB4	136	56	17	64	132	29	15	88
	20-OH-LTB4	46	0	0	46	27	0	0	27
	6-trans-TB4	25	0	0	25	8	0	0	8
	LTB3	58	0	0	58	29	0	0	29
	LTB4	59	0	0	59	36	0	0	36
	LTC4	6	0	0	6	0	0	0	0
	LTD4	3	0	0	3	0	0	0	0
	LTE4	0	0	0	0	0	0	0	0
	LXA4	0	0	0	0	0	0	0	0
	PGB2	80	69	0	11	79	60	0	19
	PGD1	0	0	0	0	0	0	0	0
	PGD2	0	0	0	0	0	0	0	0
	PGD3	2	2	0	0	0	0	0	0
	PGE1	31	19	0	13	39	22	0	17
	PGE2	15	5	0	10	23	5	0	18
	PGE3	15	5	0	10	23	5	0	18
	6-keto-PGF1α	49	21	0	29	55	10	0	45
	PGF2α	133	0	0	133	118	0	0	118

(Continues)

Table 3 Continued

	100 mg column				500 mg column			
	Total recovery (%)	Recovery per fraction (%)[a]			Total recovery (%)	Recovery per fraction (%)[a]		
		In FFA (%)	In NL (%)	In PL (%)		In FFA (%)	In NL (%)	In PL (%)
PGJ2	52	40	0	11	49	39	0	10
15-deoxy-PGJ2	55	50	0	5	53	46	0	7
TXB2	0	0	0	0	0	0	0	0
Resolvin E1	39	0	0	39	11	0	0	11
9,10,13-TriHOME	85	8	0	77	88	11	0	77
9,12,13-TriHOME	74	4	0	70	75	4	0	71

Abbreviations: FFA, unesterified fatty acids; NL, neutral lipids; PL, phospholipids; EpOME, epoxyoctadecenoic acid; EpETrE, epoxyeicosatrienoic acid; EpETE, epoxyeicosatetraenoic acid; EpDPE, epoxydocosapentaenoic acid; DiHOME, dihydroxyoctadecenoic acid; DiHETrE, dihydroxyeicosatrienoic acid; DiHETE, dihydroxyeicosatetraenoic acid; HODE, hydroxyoctadecadienoic acid; HETrE, hydroxyeicosatrienoic acid; HETE, hydroxyeicosatetraenoic acid; HOTrE, hydroxyoctadecatrienoic acid; HEPE, hydroxyeicosapentaenoic acid; HDoHE, hydroxydocosahexaenoic acid; LT, leukotriene; LX, lipoxin; PG, prostaglandins; TX, thromboxane; TriHOME, trihydroxyoctadecenoic acid; TXB2, tromboxane B2.

[a]Calculated based on the corrected recovery.

not statistically differ between the 100 and 500 mg columns. The only detected EPA-derived metabolite, 14(15)-EpETE, was 10 times lower in PL separated with the 500 mg column compared to the 100 mg column ($p < 0.05$).

Concentrations of several LNA-derived metabolites (9(10)- and 12(13)-EpOME, 9,10- and 12,13-DiHOME, 9- and 13-HODE, 9-oxo-octadecadienoic acid [oxo-ODE]), ARA-derived hydroxylated metabolites (HETE), and EPA-derived hydroxylated compounds (15-HEPE) were significantly lower in NL and PL by 23–96% with the 500 mg column compared to the 100 mg column. It is not clear why these differences were found between the 100 and 500 mg columns. The lack of esterified analytical standards makes it difficult to know whether the concentration differences were due to losses during the column separation or ion suppression.

Overall, our data indicate that the 500 mg column reliably separates esterified epoxides of ARA and DHA because (1) many unesterified long-chain PUFA epoxides did not coelute with esterified NL and PL when using the 500 mg column compared to the 100 mg column (Table 3), and (2) although rat brain ARA and DHA epoxide concentrations were statistically similar between the two columns, the coefficient of variation was lower with the 500 mg column, suggesting better reproducibility (Table 4). Thus, the 500 mg column was used to test the effects of hypercapnia/ischemia on brain-esterified ARA and DHA epoxide concentrations (following section).

Hypercapnia-Ischemia Study

Data showing the percent of ARA-, EPA-, and DHA-derived epoxides detected in brain PL and NL of each of the MW-irradiated and CO_2-asphyxiated groups are shown in Supplementary Table 5. As shown, most of the frequently detected compounds were ARA- and DHA-derived epoxides.

Means and SD, as well as medians and interquartile ranges, of ARA and DHA epoxides within PL and NL are presented in Supplementary Table 6. Published values for corresponding free oxylipins from the same rats are also presented in Supplementary Table 6 (Hennebelle et al., 2019).

The data for PL-bound epoxides of ARA and DHA were highly variable and not normally distributed (Supplementary Table 6). Statistical analysis by Mann–Whitney U test showed no significant differences in PL-bound epoxides between the MW-irradiated and CO_2-asphyxiated groups ($p > 0.05$).

NL-bound ARA epoxides were normally distributed and therefore analyzed by unpaired *t*-test; NL-bound DHA epoxides failed the normality of distribution test (in the

Table 4 Brain oxylipin concentrations (pmol/g) in NL and PL separated post-Folch extraction with the 100 and 500 mg aminopropyl columns. The brain was from one rat euthanized by CO_2-induced hypercapnia/ischemia

		100 mg column				500 mg column			
		NL fraction		PL fraction		NL fraction		PL fraction	
		Concentration	CV (%)	Concentration	CV (%)	Concentration	CV (%)	Concentration	CV (%)
Epoxy-	**9(10)-EpOME**	1262.6 ± 113.9	9	951.0 ± 159.7	17	533.4 ± 83.0*	16	504.1 ± 27.1*	5
	12(13)-EpOME	3001.5 ± 194.4	6	1511.1 ± 320.7	21	1158.9 ± 134.5*	12	350.5 ± 16.5*	5
	5(6)-EpETrE	ND	—	1378.7 ± 615.9	45	ND	—	1477.3 ± 287.5	19
	8(9)-EpETrE	ND	—	1591.9 ± 616.6	39	12.8 ± 2.9	23	822.1 ± 74.5	9
	11(12)-EpETrE	ND	—	1336.2 ± 483.2	36	14.2, 15.6		1276.9 ± 191.1	15
	14(15)-EpETrE	ND	—	4728.4 ± 2570.5	54	20.0, 22.0		3899.0 ± 341.8	9
	8(9)-EpETE	ND	—	235.8	—	ND	—	ND	—
	11(12)-EpETE	ND	—	72.0	—	ND	—	16.0	—
	14(15)-EpETE	ND	—	137.6 ± 76.5	56	ND	—	13.8 ± 3.1*	22
	17(18)-EpETE	ND	—	1826.6	—	ND	—	125.3	—
	7(8)-EpDPE	ND	—	2719.2 ± 1089.0	40	ND	—	1903.2 ± 262.6	14
	10(11)-EpDPE	14.9	—	2947.9 ± 1176.0	40	12.8 ± 2.9	22	2068.7 ± 190.0	9
	13(14)-EpDPE	ND	—	3612.9 ± 1543.6	43	28.5, 10.3		2773.3 ± 282.9	10
	16(17)-EpDPE	ND	—	3722.1 ± 1779.8	48	ND	—	3051.2 ± 325.0	11
	19(20)-EpDPE	ND	—	5971.6 ± 2522.9	42	ND	—	2646.0 ± 78.5	3
Dihydroxy-	**9,10-DiHOME**	45.0 ± 3.4	7	161.9 ± 22.1	14	18.5 ± 3.0*	16	66.4 ± 6.1*	9
	12,13-DiHOME	60.3, 29.3		245.6 ± 28.3	12	26.5 ± 3.5	13	124.6 ± 18.3*	15
	5,6-DiHETrE	ND	—	439.0 ± 183.7	42	ND	—	503.9 ± 56.0	11
	8,9-DiHETrE	ND	—	55.4	—	ND	—	38.0, 30.4	
	11,12-DiHETrE	ND	—	ND	—	ND	—	23.6 ± 11.4	48
	14,15-DiHETrE	ND	—	36.5 ± 11.0	30	ND	—	43.0 ± 16.8	39
	8,15-DiHETE	ND	—	ND	—	ND	—	169.0 ± 18.3	11
Hydroxy-	**9-HODE**	1348.2 ± 307.4	23	1434.9 ± 321.5	22	165.4 ± 43.6*	26	162.3 ± 45.6*	28
	13-HODE	1563.0 ± 461.6	30	1772.0 ± 468.0	26	284.3 ± 158.4*	56	240.5 ± 128.7*	54
	15(S)-HETrE	ND	—	ND	—	ND	—	8.0, 8.5	
	5-HETE	ND	—	261.3 ± 28.0	11	ND	—	145.3 ± 8.0*	5
	8-HETE	ND	—	108.1 ± 21.2	20	ND	—	61.3 ± 0.1*	0
	11-HETE	ND	—	151.0 ± 35.6	24	ND	—	70.2 ± 5.1*	7
	12-HETE	ND	—	95.5 ± 13.3	14	ND	—	73.5 ± 21.2	29
	15-HETE	ND	—	253.7 ± 82.4	32	ND	—	166.2 ± 33.7	20
	20-HETE	ND	—	1151.9, 836.6		ND	—	125.4, 109.3	
	5-HEPE	640.9, 103.2		866.6 ± 573.8	66	ND	—	34.2 ± 13.2	38
	8-HEPE	137.2	—	627.4 ± 399.7	64	ND	—	23.6 ± 4.3	18
	12-HEPE	1206.3, 894.1		6859.7 ± 5002.9	73	221.8, 58.6		1170.6 ± 351.2	30
	15-HEPE	317.4	—	1883.9 ± 709.6	38	ND	—	601.8 ± 121.5*	20
Ketones, LTB	**9-oxo-ODE**	364.8 ± 121.2	33	448.7 ± 95.1	21	74.8 ± 29.8*	40	38.3 ± 15.5*	41
	13-oxo-ODE	ND	—	614.0	—	ND	—	62.1	—
	15-oxo-ETE	ND	—	27.1, 43.8		ND	—	16.2, 21.2	
	20-COOH-LTB4	387.0 ± 57.3	15	314.1, 253.7		69.0 ± 6.6*	10	n.d.	—

Data are mean ± SD (n = 3/column). Raw values are presented for oxylipins detected in one or two of three samples.

Abbreviations: ND, not detected; NL, neutral lipids; PL, phospholipids; EpOME, epoxyoctadecenoic acid; EpETrE, epoxyeicosatrienoic acid; EpETE, epoxyeicosatetraenoic acid; EpDPE, epoxydocosapentaenoic acid; DiHOME, dihydroxyoctadecenoic acid; DiHETrE, dihydroxyeicosatrienoic acid; DiHETE, dihydroxyeicosatetraenoic acid; HODE, hydroxyoctadecadienoic acid; HETrE, hydroxyeicosatrienoic acid; HETE, hydroxyeicosatetraenoic acid; HOTrE, hydroxyoctadecatrienoic acid; HEPE, hydroxyeicosapentaenoic acid; HDoHE, hydroxydocosahexaenoic acid; LT, leukotriene.

*$p < 0.05$ between 100 and 500 mg columns per lipid fraction by unpaired t-test.

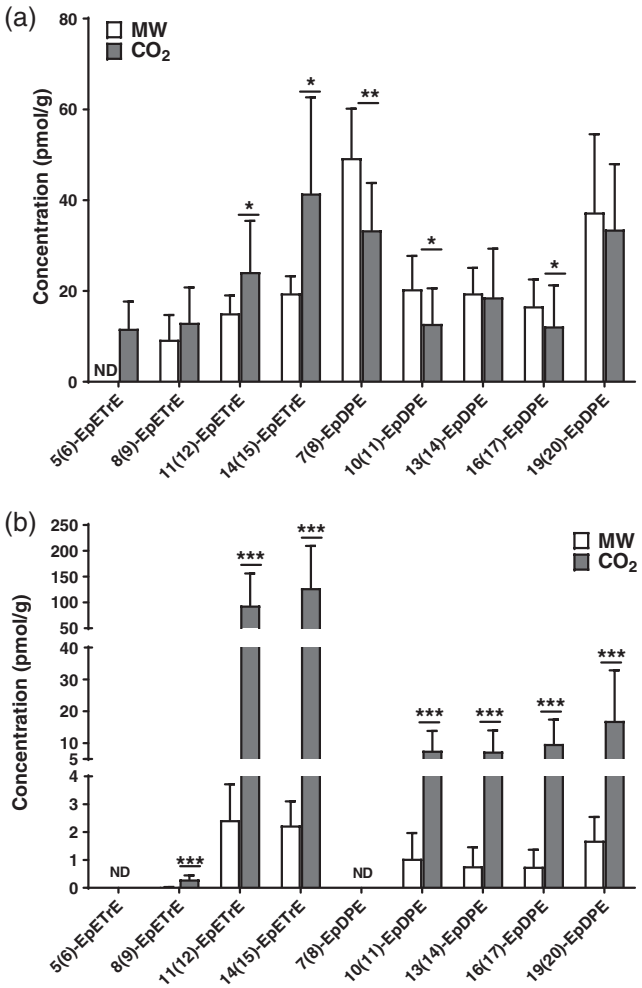

Fig. 1 Concentration of arachidonic acid (ARA)- and docosahexaenoic acid (DHA)-derived epoxides in (a) neutral lipids (NL) and (b) unesterified fatty acids (FFA) (adapted from Hennebelle et al. (2019)) of rats subjected to head-focused microwave fixation (MW) or CO_2-induced hypercapnia/ischemia (CO_2). Data are mean ± SD ($n = 8$ per group). *$p < 0.05$; **$p < 0.01$; ***$p < 0.001$ (Unpaired *t*-test or Mann–Whitney U test). Abbreviations: EpETrE, epoxyeicosatrienoic acid; EpDPE, epoxydocosapentaenoic acid; ND, not detected

CO_2 group only), so a Mann–Whitney U test was used. Fig. 1a shows mean (±SD) PUFA epoxide concentrations in brain NL of rats subjected to high-energy microwave fixation (controls) and CO_2-induced hypercapnia/ischemia (mean and median values also provided in Supplementary Table 6). As shown, brain concentrations of ARA-derived 11(12)- and 14(15)-EpETrE were significantly increased in the CO_2 group, compared to MW controls, by 60% and 112%, respectively (Fig. 1a; $p < 0.05$ by unpaired *t*-test). DHA-derived 7(8)-EpDPE, 10(11)-EpDPE, and 16(17)-EpDPE were significantly decreased by 32%, 37%, and 27%, respectively, in the CO_2 group compared to MW controls ($p < 0.05$ by Mann–Whitney U test; Fig. 1a).

Published mean values of unesterified ARA and DHA epoxide concentrations measured in the second hemisphere of the same rats are shown in Fig. 1b (Hennebelle et al., 2019). For these measurements, the brains were extracted with methanol, purified with Oasis HLB columns, and analyzed with UPLC–MS/MS as reported (Hennebelle et al., 2019). 8(9)-EpETrE was analyzed by an unpaired *t*-test because it was normally distributed, whereas other metabolites were analyzed by Mann–Whitney U because they were not normally distributed in one or two groups. As shown in Fig. 1b, unesterified ARA- and DHA-derived epoxides were significantly higher by 7–57-fold following CO_2-induced hypercapnia/ischemia relative to microwave fixation. Unesterified 7(8)-EpDPE, while present in PL and NL, was not detected in the free oxylipin pool.

Pathway Depiction

Fig. 2 depicts plausible pathways that regulate the turnover of fatty acid epoxides within rat brain lipids. As shown, PUFA-derived epoxides can be liberated from membrane PL or NL *via* lipase enzymes and re-esterified *via* acyl-CoA synthetase and acyltransferase enzymes. Specific

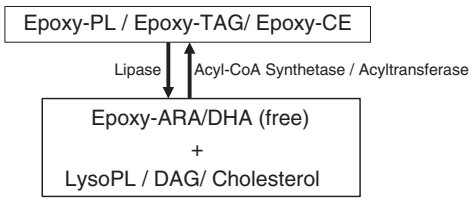

Fig. 2 Pathways regulating the turnover of fatty acid epoxides within rat brain lipids. As shown, polyunsaturated fatty acids (PUFA)-derived epoxides can be liberated from membrane phospholipids (PL) or neutral lipids (NL) *via* lipase enzymes and re-esterified *via* acyl-CoA synthetase and acyltransferase enzymes. The acylation of free epoxy-ARA or epoxy-DHA (via acyl synthetases) enables their esterification to lysophospholipids (LysoPL), diacylglycerols (DAG) or cholesterol via acyltransferase enzymes. This generates epoxy-PL/TAG/CE (i.e. a PL, TAG or CE containing epoxidized ARA or DHA). LysoPL can also be directly oxidized by LOX, and then esterified to a saturated fatty acid as recently described by Liu et al., 2019. The observed increase in arachidonic acid (ARA)-derived epoxides and reduction in docosahexaenoic acid (DHA)-derived epoxides during hypercapnia/ischemia could be explained by changes in acyl synthethase/acyltranferase-mediated esterification and/or lipase-mediated release

enzyme isoforms that regulate this pathway remain to be determined, although Acyl-CoA synthetase 4 was shown to incorporate EpETrE into PL (Klett et al., 2017).

Discussion

In the present study, we validated an aminopropyl column method for separating PL- and NL-bound epoxides of long-chain PUFA and demonstrated that hypercapnia/ischemia altered ARA and DHA epoxides within NL. Specifically, the concentrations of two ARA-derived epoxides (11(12)- and 14(15)-EpETrE) were increased by 60–112%, and three DHA-derived epoxides (7(8)-EpDPE, 10(11)-EpDPE and 16(17)-EpDPE) were decreased by 27–37% in brain NL of rats subjected to CO_2-induced hypercapnia/ischemia compared to MW-irradiated controls. This suggests the presence of a turnover pathway that regulates ARA and DHA epoxide levels within NL (Fig. 2).

With regard to the aminopropyl separation method, FFA, PL, and NL standards separated well with the 500 mg column (Table 2). Unesterified PUFA-derived hydroxy, epoxy, and ketone oxylipin standards applied to both columns eluted with the FFA pool as expected despite the low recovery for some alcohol and ketone compounds (Table 3), possibly due to degradation or elution during one of the wash steps listed in Table 1. The elution of unesterified hydroxy, epoxy, and ketone oxylipins with the FFA pool indicates that, if present in the sample, they are not likely to coelute with PL or NL.

Both 100 and 500 mg columns had some fatty acid contaminants in them despite being washed with organic solvents and acid. LNA and ALA (but not other PUFA) contaminants present in NL, PL, and FFA and separated by the 100 and 500 mg columns (Supplementary Table 4) might produce LNA- and ALA-derived oxylipin artifacts. This is why we chose to focus on ARA-, EPA-, and DHA-derived oxylipins, as metabolites of LNA and ALA cannot be reliably quantified after column separation.

The separation of brain total lipids using both 100 and 500 mg columns yielded comparable results for ARA- and DHA-derived epoxides, although the variance was lower, and the number of detected compounds was higher when the extracted lipids were separated using the 500 mg column relative to the 100 mg column (Table 4). EPA-derived epoxides were rarely detected with either column. Differences in column recovery for other compounds (e.g. hydroxy and ketone PUFA metabolites) are difficult to explain in the absence of authentic esterified oxylipin standards. Thus, only ARA- and DHA-derived epoxides bound to NL and PL were considered reliable to quantify using the 500 mg column.

The 60–112% increase in ARA-derived epoxides in brain NL of rats subjected to CO_2-induced hypercapnia/ischemia relative to microwave-irradiated controls (Fig. 1a) could be due to increased free ARA-epoxide esterification, decreased lipase-mediated release of epoxy ARA bound to NL, or direct epoxidation of ARA esterified to NL. Increased free ARA-epoxide esterification is a likely mechanism explaining the increase in ARA-epoxide in NL because of the observed increase in free ARA-epoxide concentrations following CO_2-induced hypercapnia/ischemia (Fig. 1b). Free ARA epoxides are substrates for acylation and esterification by acyl CoA synthetase and acyltransferase, respectively (Klett et al., 2017). A reduction in lipase-mediated release is unlikely because the concentration of unesterified epoxy-ARA metabolites was increased in the CO_2-asphyxiated group compared to microwave controls (Fig. 1b). Notably, the hydroxylation of PL was reported to occur *in vitro* (Chaitidis et al., 1998) and in peripheral immune cells *via* LOX (Slatter et al., 2018; Uderhardt et al., 2017), but to our knowledge, direct epoxidation of esterified PUFA (to NL) has not been demonstrated. Future studies should resolve the mechanisms of esterified epoxide ARA formation in NL *in vivo*.

DHA-derived 7(8)-EpDPE was lower in brain NL of CO_2-asphyxiated rats compared to MW controls. Unesterified 7(8)-EpDPE was not detected (Hennebelle et al., 2019). It is possible that 7(8)-EpDPE is selectively retained in PL and NL. The decrease in its concentration within NL following ischemia/hypercapnia could be due to (1) its conversion into diols within NL *via* epoxide hydrolase or (2) rapid lipase-mediated release and degradation *via* sEH. These hypotheses should be tested once better assays for esterified diols within PL and NL become available.

DHA-derived 10(11)-EpDPE and 16(17)-EpDPE were also lower in NL of CO_2-asphyxiated rats compared to MW controls but were higher in the free pool. The decrease in NL-bound DHA epoxides (and concomitant increase in unesterified concentrations) could be due to increased lipase-mediated hydrolysis from NL-bound epoxides during hypercapnia/ischemia. However, given the magnitude of changes in free versus NL-bound 10(11)-EpDPE and 16(17)-EpDPE (Fig. 1), CYP-mediated synthesis of unesterified DHA epoxides (from free DHA) likely explains the increase in their concentration during hypercapnia/ischemia.

Previously, we reported that up to approximately 90% of oxylipins in the brain are esterified to complex lipids, but the lipid species to which they are bound have not been characterized (Taha et al., 2018). In the present study, we demonstrated that the majority of oxylipins were esterified to PL (Table 3; Supplementary Table 6). Quantitatively, PL-bound ARA and DHA epoxides, although variable, were approximately 39–214 more abundant (across the two groups) than NL-bound epoxides. NL PUFA epoxides were similar in concentration to unesterified oxylipins (Fig. 1). These observations reflect *in vivo* regulatory pathways that control oxylipin turnover (esterification and release) within brain lipid pools, particularly during hypercapnia/ischemia, as proposed in Fig. 2. This turnover pathway could regulate free oxylipin availability alongside other established pathways involving lipase-mediated release of PUFA from esterified lipid pools and their oxidation *via* CYP, LOX, COX, or other enzymes to form free oxylipins.

The variability in brain-oxidized PL was high (Supplementary Table 6). It is unlikely that this was due to the SPE fractionation process because none of the unesterified epoxides of interest eluted with PL (Table 3), and the authentic standard (1,2-dipalmitoyl-sn-glycero-3-phosphocholine) separated well with the 500 mg column used in the rodent study (Table 2). Oxidized PL, however, are slightly more polar than nonoxidized PL. Hence, one explanation of the variability could be partial loss of oxidized PL within the aqueous phase of the Folch extract. Another explanation is that a small but non-trivial amount of free oxylipins coeluted with oxidized PL due to their similar polarities. In the absence of oxidized PL authentic standards, these scenarios cannot be verified. Notably, the variability in oxidized PL was low when the same sample was analyzed thrice (technical replicates; Table 3). This points to the possibility that the variability could be biological, arising from the rapid remodeling of epoxide PL. The half-lives and remodeling rates of epoxidized PL in the brain are not known.

CO_2 asphyxiation is a common euthanasia technique. Thus, the observed changes in NL-bound epoxides following CO_2 asphyxiation have implications on other studies using this technique as a euthanasia method. Compared to MW-irradiated controls, the magnitude of changes following CO_2 asphyxiation was smaller in NL (27–112%, Fig. 1) than in free oxylipins, where increases of up to 155-fold were observed (Hennebelle et al., 2019). This indicates that postmortem ischemia minimally impacts the esterified PUFA-epoxide pool compared to the unesterified pool, suggesting that it can be used as a more reliable marker of disturbed brain oxylipin metabolism.

A limitation of this study is that regional changes in esterified oxylipins were not explored, because measurements were taken from whole brain. It would be worthwhile to examine ischemia-induced changes in esterified oxylipins across brain regions and cell types (glia vs neurons) to better understand vulnerable brain areas or cell populations. In addition, the contribution of esterified oxylipins originating from peripheral blood vessels is not known. Hypercapnia/ischemia is known to increase blood flow to the brain, which means that the changes seen in esterified oxylipins could originate, in part, from peripheral blood. Finally, it should be noted that base hydrolysis of esterified oxylipins at 60 °C could potentially generate oxidation artifacts. Determining the contribution of such artifacts to the biological signal using authentic esterified standards (when they become commercially available) would be paramount to confirming our results.

In summary, this study provides new *in vivo* evidence that acute brain injury induced by hypercapnia/ischemia increases ARA epoxides and decreases DHA epoxides esterified to NL, in parallel to the recently described increases in unesterified ARA and DHA epoxides (Hennebelle et al., 2019). These findings suggest an active turnover pathway involved in transporting unesterified ARA- and DHA-derived epoxides within esterified lipid compartments in rat brain. The enzymatic machinery regulating this process remains to be characterized. As ARA- and DHA-derived epoxides are important mediators of cerebral vascular tone with anti-inflammatory and proresolving properties (reviewed by Swardfager et al., 2018), identifying and targeting the enzymes involved in their turnover within NL provides new potential for treating ischemic or other types of brain injury.

Acknowledgement This study was supported by the Hellman Family Foundation (AYT) and Natural Sciences and Engineering Research Council of Canada (grant #482597, R.P.B.). Additional support was provided by the National Institutes of Health (U24-DK097154; J.W.N.) and the USDA (2032-51530-022-00D, J.W.N.), NIEHS/R01 ES002710 (B.D.H.), and NIEHS/Superfund Research Program P42 ES004699 (B.D.H.). The USDA is an equal opportunity provider and employer. Y.O. is a recipient of a fellowship from the JSPS Core-to-Core Program (Advanced Research Networks) entitled "Establishment of international agricultural immunology research-core for a quantum improvement in food safety." The authors thank Dr. Dmitry Grapov for his efforts in developing the oxygenated complex lipid separation

method, Dr. Marie Hennebelle for assistance with the method validation, and Dr. Alex Kitson for assistance with the animal experiments.

Conflict of Interest The authors declare that they have no conflicts of interest.

Author Contributions A.Y.T. conceived the concept and hypothesis surrounding oxylipin esterification into brain lipid pools during brain injury. A.Y.T., R.P.B., and A.H.M. designed the experiments. A.H.M. conducted the animal experiments. J.W.N. and T.P. guided and advised on the esterified lipid separation method. Y.O. analyzed the rat brain samples and contributed to the interpretation. A.Y.T., A.H.M., R.P.B., B.D.H., and J.Y. designed or performed prior pilot studies leading up to the present study. A.Y.T. wrote the article. All authors reviewed and approved the manuscript.

References

Abdu, E., Bruun, D. A., Yang, D., Yang, J., Inceoglu, B., Hammock, B. D., … Lein, P. J. (2011) Epoxyeicosatrienoic acids enhance axonal growth in primary sensory and cortical neuronal cell cultures. *Journal of Neurochemistry*, **117**:632–642.

Arnold, C., Markovic, M., Blossey, K., Wallukat, G., Fischer, R., Dechend, R., … Schunck, W. H. (2010) Arachidonic acid-metabolizing cytochrome P450 enzymes are targets of {omega}-3 fatty acids. *The Journal of Biological Chemistry*, **285**: 32720–32733.

Bazan Jr., N. G. (1970) Effects of ischemia and electroconvulsive shock on free fatty acid pool in the brain. *Biochimica et Biophysica Acta*, **218**:1–10.

Bernstrom, K., Kayganich, K., Murphy, R. C., & Fitzpatrick, F. A. (1992) Incorporation and distribution of epoxyeicosatrienoic acids into cellular phospholipids. *The Journal of Biological Chemistry*, **267**:3686–3690.

Brezinski, M. E., & Serhan, C. N. (1990) Selective incorporation of (15S)-hydroxyeicosatetraenoic acid in phosphatidylinositol of human neutrophils: Agonist-induced deacylation and transformation of stored hydroxyeicosanoids. *Proceedings of the National Academy of Sciences of the United States of America*, **87**: 6248–6252.

Chaitidis, P., Schewe, T., Sutherland, M., Kuhn, H., & Nigam, S. (1998) 15-Lipoxygenation of phospholipids may precede the sn-2 cleavage by phospholipases A2: Reaction specificities of secretory and cytosolic phospholipases A2 towards native and 15-lipoxygenated arachidonoyl phospholipids. *FEBS Letters*, **434**: 437–441.

Chang, J., Jiang, L., Wang, Y., Yao, B., Yang, S., Zhang, B., & Zhang, M. Z. (2015) 12/15 Lipoxygenase regulation of colorectal tumorigenesis is determined by the relative tumor levels of its metabolite 12-HETE and 13-HODE in animal models. *Oncotarget*, **6**:2879–2888.

Dabertrand, F., Hannah, R. M., Pearson, J. M., Hill-Eubanks, D. C., Brayden, J. E., & Nelson, M. T. (2013) Prostaglandin E2, a postulated astrocyte-derived neurovascular coupling agent, constricts rather than dilates parenchymal arterioles. *Journal of Cerebral Blood Flow and Metabolism*, **33**:479–482.

Fang, X., Weintraub, N. L., & Spector, A. A. (2003) Differences in positional esterification of 14,15-epoxyeicosatrienoic acid in phosphatidylcholine of porcine coronary artery endothelial and smooth muscle cells. *Prostaglandins & Other Lipid Mediators*, **71**:33–42.

Fer, M., Corcos, L., Dreano, Y., Plee-Gautier, E., Salaun, J. P., Berthou, F., & Amet, Y. (2008a) Cytochromes P450 from family 4 are the main omega hydroxylating enzymes in humans: CYP4F3B is the prominent player in PUFA metabolism. *Journal of Lipid Research*, **49**:2379–2389.

Fer, M., Dreano, Y., Lucas, D., Corcos, L., Salaun, J. P., Berthou, F., & Amet, Y. (2008b) Metabolism of eicosapentaenoic and docosahexaenoic acids by recombinant human cytochromes P450. *Archives of Biochemistry and Biophysics*, **471**:116–125.

Folch, J., Lees, M., & Sloane Stanley, G. H. (1957) A simple method for the isolation and purification of total lipides from animal tissues. *The Journal of Biological Chemistry*, **226**:497–509.

Funk, C. D. (2001) Prostaglandins and leukotrienes: Advances in eicosanoid biology. *Science*, **294**:1871–1875.

Ge, R. S., Chen, G. R., Dong, Q., Akingbemi, B., Sottas, C. M., Santos, M., … Hardy, M. P. (2007) Biphasic effects of postnatal exposure to diethylhexylphthalate on the timing of puberty in male rats. *Journal of Andrology*, **28**:513–520.

Grapov, D (2012) *Application of targeted metabolomic profiling and multivariate data analysis for the study of nutrition and disease*. (Thesis Dissertation: 30–101). University of California Davis.

Greene, J. F., Newman, J. W., Williamson, K. C., & Hammock, B. D. (2000) Toxicity of epoxy fatty acids and related compounds to cells expressing human soluble epoxide hydrolase. *Chemical Research in Toxicology*, **13**:217–226.

Hennebelle, M., Metherel, A. H., Kitson, A. P., Otoki, Y., Yang, J., Lee, K. S. S., … Taha, A. Y. (2019) Brain oxylipin concentrations following hypercapnia/ischemia: Effects of brain dissection and dissection time. *Journal of Lipid Research*, **60**:671–682.

Hennebelle, M., Zhang, Z., Metherel, A. H., Kitson, A. P., Otoki, Y., Richardson, C. E., … Taha, A. Y. (2017) Linoleic acid participates in the response to ischemic brain injury through oxidized metabolites that regulate neurotransmission. *Scientific Reports*, **7**:4342.

Inceoglu, A. B., Clifton, H. L., Yang, J., Hegedus, C., Hammock, B. D., & Schaefer, S. (2012) Inhibition of soluble epoxide hydrolase limits niacin-induced vasodilation in mice. *Journal of Cardiovascular Pharmacology*, **60**:70–75.

Inceoglu, B., Schmelzer, K. R., Morisseau, C., Jinks, S. L., & Hammock, B. D. (2007) Soluble epoxide hydrolase inhibition reveals novel biological functions of epoxyeicosatrienoic acids (EETs). *Prostaglandins & Other Lipid Mediators*, **82**:42–49.

Joulain, C., Meskini, N., Anker, G., Lagarde, M., & Prigent, A. F. (1995) Esterification of 12(S)-hydroxy-5,8,10,14-eicosatetraenoic acid into the phospholipids of human peripheral blood mononuclear cells: Inhibition of the proliferative response. *Journal of Cellular Physiology*, **164**:154–163.

Klett, E. L., Chen, S., Yechoor, A., Lih, F. B., & Coleman, R. A. (2017) Long-chain acyl-CoA synthetase isoforms differ in preferences for eicosanoid species and long-chain fatty acids. *Journal of Lipid Research*, **58**:884–894.

Lahvic, J. L., Ammerman, M., Li, P., Blair, M. C., Stillman, E. R., Fast, E. M., … Zon, L. I. (2018) Specific oxylipins enhance vertebrate hematopoiesis via the receptor GPR132. *Proceedings of the National Academy of Sciences of the United States of America*, **115**:9252–9257.

Lands, W. E., & Merkl, I. (1963) Metabolism of glycerolipids. III. Reactivity of various acyl esters of coenzyme A with alpha'-acylglycerophosphorylcholine, and positional specificities in lecithin synthesis. *The Journal of Biological Chemistry*, **238**:898–904.

Laneuville, O., Breuer, D. K., Xu, N., Huang, Z. H., Gage, D. A., Watson, J. T., … Smith, W. L. (1995) Fatty acid substrate specificities of human prostaglandin-endoperoxide H synthase-1 and -2. Formation of 12-hydroxy-(9Z, 13E/Z, 15Z)- octadecatrienoic acids from alpha-linolenic acid. *The Journal of Biological Chemistry*, **270**:19330–19336.

Levy, B. D., Clish, C. B., Schmidt, B., Gronert, K., & Serhan, C. N. (2001) Lipid mediator class switching during acute inflammation: Signals in resolution. *Nature Immunology*, **2**:612.

Liu, G. Y., Moon, S. H., Jenkins, C. M., Sims, H. F., Guan, S., & Gross, R. W. (2019) Synthesis of oxidized phospholipids by sn-1 acyltransferase using 2-15-HETE lysophospholipids. *The Journal of Biological Chemistry*, **294**:10146–10159.

Liu, X., Li, C., Gebremedhin, D., Hwang, S. H., Hammock, B. D., Falck, J. R., … Koehler, R. C. (2011) Epoxyeicosatrienoic acid-dependent cerebral vasodilation evoked by metabotropic glutamate receptor activation in vivo. *American Journal of Physiology. Heart and Circulatory Physiology*, **301**:H373–H381.

Morrow, J. D., Awad, J. A., Kato, T., Takahashi, K., Badr, K. F., Roberts 2nd, L. J., & Burk, R. F. (1992) Formation of novel non-cyclooxygenase-derived prostanoids (F2-isoprostanes) in carbon tetrachloride hepatotoxicity. An animal model of lipid peroxidation. *Journal of Clinical Investigation*, **90**:2502–2507.

Murphy, E., Glasgow, W., Fralix, T., & Steenbergen, C. (1995) Role of lipoxygenase metabolites in ischemic preconditioning. *Circulation Research*, **76**:457–467.

Obinata, H., Hattori, T., Nakane, S., Tatei, K., & Izumi, T. (2005) Identification of 9-hydroxyoctadecadienoic acid and other oxidized free fatty acids as ligands of the G protein-coupled receptor G2A. *The Journal of Biological Chemistry*, **280**:40676–40683.

Orr, S. K., Palumbo, S., Bosetti, F., Mount, H. T., Kang, J. X., Greenwood, C. E., … Bazinet, R. P. (2013) Unesterified docosahexaenoic acid is protective in neuroinflammation. *Journal of Neurochemistry*, **127**:378–393.

Ramadan, E., Basselin, M., Taha, A. Y., Cheon, Y., Chang, L., Chen, M., & Rapoport, S. I. (2011) Chronic valproate treatment blocks D2-like receptor-mediated brain signaling via arachidonic acid in rats. *Neuropharmacology*, **61**:1256–1264.

Rand, A. A., Barnych, B., Morisseau, C., Cajka, T., Lee, K. S. S., Panigrahy, D., & Hammock, B. D. (2017) Cyclooxygenase-derived proangiogenic metabolites of epoxyeicosatrienoic acids. *Proceedings of the National Academy of Sciences of the United States of America*, **114**:4370–4375.

Rapoport, S. I. (1996) In vivo labeling of brain phospholipids by long-chain fatty acids: Relation to turnover and function. *Lipids*, **31**:S97–S101.

Rey, C., Nadjar, A., Buaud, B., Vaysse, C., Aubert, A., Pallet, V., … Joffre, C. (2016) Resolvin D1 and E1 promote resolution of inflammation in microglial cells in vitro. *Brain, Behavior, and Immunity*, **55**:249–259.

Robinson, P. J., & Rapoport, S. I. (1989) A method for examining turnover and synthesis of palmitate-containing brain lipids in vivo. *Clinical and Experimental Pharmacology & Physiology*, **16**: 701–714.

Serhan, C. N., Hong, S., Gronert, K., Colgan, S. P., Devchand, P. R., Mirick, G., & Moussignac, R. L. (2002) Resolvins: A family of bioactive products of omega-3 fatty acid transformation circuits initiated by aspirin treatment that counter proinflammation signals. *The Journal of Experimental Medicine*, **196**:1025–1037.

Slatter, D. A., Percy, C. L., Allen-Redpath, K., Gajsiewicz, J. M., Brooks, N. J., Clayton, A., … O'Donnell, V. B. (2018) Enzymatically oxidized phospholipids restore thrombin generation in coagulation factor deficiencies. *JCI Insight*, **3**(6): e98459.

Snyder, N. W., Golin-Bisello, F., Gao, Y., Blair, I. A., Freeman, B. A., & Wendell, S. G. (2015) 15-Oxoeicosatetraenoic acid is a 15-hydroxyprostaglandin dehydrogenase-derived electrophilic mediator of inflammatory signaling pathways. *Chemico-Biological Interactions*, **234**:144–153.

Stenson, W. F., & Parker, C. W. (1979a) 12-L-hydroxy-5,-8,10,14-eicosatetraenoic acid, a chemotactic fatty acid, is incorporated into neutrophil phospholipids and triglyceride. *Prostaglandins*, **18**:285–292.

Stenson, W. F., & Parker, C. W. (1979b) Metabolism of arachidonic acid in ionophore-stimulated neutrophils. Esterification of a hydroxylated metabolite into phospholipids. *The Journal of Clinical Investigation*, **64**:1457–1465.

Swardfager, W., Hennebelle, M., Yu, D., Hammock, B. D., Levitt, A. J., Hashimoto, K., & Taha, A. Y. (2018) Metabolic/inflammatory/vascular comorbidity in psychiatric disorders; soluble epoxide hydrolase (sEH) as a possible new target. *Neuroscience and Biobehavioral Reviews*, **87**:56–66.

Taha, A. Y., Chang, L., Chen, M., Rapoport, S. I., & Ramadan, E. (2014) D2-like receptor activation does not initiate a brain docosahexaenoic acid signal in unanesthetized rats. *BMC Neuroscience*, **15**:113.

Taha, A. Y., Hennebelle, M., Yang, J., Zamora, D., Rapoport, S. I., Hammock, B. D., & Ramsden, C. E. (2018) Regulation of rat plasma and cerebral cortex oxylipin concentrations with increasing levels of dietary linoleic acid. *Prostaglandins, Leukotrienes, and Essential Fatty Acids*, **138**:71–80.

Trepanier, M. O., Taha, A. Y., Mantha, R. L., Ciobanu, F. A., Zeng, Q. H., Tchkhartichvili, G. M., … Burnham, W. M. (2012) Increases in seizure latencies induced by subcutaneous docosahexaenoic acid are lost at higher doses. *Epilepsy Research*, **99**: 225–232.

Uderhardt, S., Ackermann, J. A., Fillep, T., Hammond, V. J., Willeit, J., Santer, P., … Kronke, G. (2017) Enzymatic lipid oxidation by eosinophils propagates coagulation, hemostasis, and thrombotic disease. *The Journal of Experimental Medicine*, **214**: 2121–2138.

Vito, S. T., Austin, A. T., Banks, C. N., Inceoglu, B., Bruun, D. A., Zolkowska, D., … Lein, P. J. (2014) Post-exposure administration of diazepam combined with soluble epoxide hydrolase inhibition stops seizures and modulates neuroinflammation in a murine model of acute TETS intoxication. *Toxicology and Applied Pharmacology*, **281**:185–194.

Wang, L., Gill, R., Pedersen, T. L., Higgins, L. J., Newman, J. W., & Rutledge, J. C. (2009) Triglyceride-rich lipoprotein lipolysis releases neutral and oxidized FFAs that induce endothelial cell inflammation. *Journal of Lipid Research*, **50**:204–213.

Wendell, S. G., Golin-Bisello, F., Wenzel, S., Sobol, R. W., Holguin, F., & Freeman, B. A. (2015) 15-Hydroxyprostaglandin dehydrogenase generation of electrophilic lipid signaling mediators from hydroxy omega-3 fatty acids. *The Journal of Biological Chemistry*, **290**:5868–5880.